

ACCEPTED MANUSCRIPT

Breakdown of the coherence effects and Fermi liquid behavior in YbAl₃ nanoparticles

To cite this article before publication: Cristina Echevarria Bonet *et al* 2018 *J. Phys.: Condens. Matter* in press <https://doi.org/10.1088/1361-648X/aab0c7>

Manuscript version: Accepted Manuscript

Accepted Manuscript is “the version of the article accepted for publication including all changes made as a result of the peer review process, and which may also include the addition to the article by IOP Publishing of a header, an article ID, a cover sheet and/or an ‘Accepted Manuscript’ watermark, but excluding any other editing, typesetting or other changes made by IOP Publishing and/or its licensors”

This Accepted Manuscript is © 2018 IOP Publishing Ltd.

During the embargo period (the 12 month period from the publication of the Version of Record of this article), the Accepted Manuscript is fully protected by copyright and cannot be reused or reposted elsewhere.

As the Version of Record of this article is going to be / has been published on a subscription basis, this Accepted Manuscript is available for reuse under a CC BY-NC-ND 3.0 licence after the 12 month embargo period.

After the embargo period, everyone is permitted to use copy and redistribute this article for non-commercial purposes only, provided that they adhere to all the terms of the licence <https://creativecommons.org/licenses/by-nc-nd/3.0>

Although reasonable endeavours have been taken to obtain all necessary permissions from third parties to include their copyrighted content within this article, their full citation and copyright line may not be present in this Accepted Manuscript version. Before using any content from this article, please refer to the Version of Record on IOPscience once published for full citation and copyright details, as permissions will likely be required. All third party content is fully copyright protected, unless specifically stated otherwise in the figure caption in the Version of Record.

View the [article online](#) for updates and enhancements.

Breakdown of the coherence effects and Fermi liquid behavior in YbAl_3 nanoparticles

C. Echevarria-Bonet^{1,3}, D P Rojas², J I Espeso³, J Rodríguez Fernández³, L Rodríguez Fernández⁴, E Bauer⁵, S Burdin⁶, S G Magalhães⁷, L. Fernández Barquín³

¹ BCMaterials, Building No. 500, Tech. Park Biscay, 48160 Derio, Spain.

²Dpto de Estructuras y Física de Edificación. ETSAM-Universidad Politécnica de Madrid, 28040 Madrid, Spain

³Dpto. CITIMAC, Facultad de Ciencias, Universidad de Cantabria, 39005 Santander, Spain

⁴SERMET, Universidad de Cantabria, 39005 Santander, Spain

⁵Institute of Solid State Physics, TU Wien, 1040 Wien, Austria

⁶Univ. Bordeaux, LOMA, UMR 5798, F-33400 Talence, France and CNRS, LOMA, UMR 5798, F-33400 Talence, France

⁷Instituto de Física, Universidade Federal do Rio Grande do Sul, 91501-970 Porto Alegre, Brazil

E-mail: d.rojas@upm.es

Abstract. A change in the Kondo lattice behavior of bulk YbAl_3 has been observed when the alloy is shaped into nanoparticles (≈ 12 nm). Measurements of the electrical resistivity show inhibited coherence effects and deviation from the standard Fermi liquid behavior (T^2 -dependence). The results are interpreted as due to the effect of the disruption of the periodicity of the array of Kondo ions provoked by the size reduction process. Additionally, the ensemble of randomly placed nanoparticles also triggers an extra source of electronic scattering at very low temperatures (≈ 15 K) due to quantum interference effects.

Keywords: Yb nanometric alloys, Kondo lattice, single impurity, electrical resistivity, Quantum interference effects

Submitted to: *J. Phys.: Condens. Matter*

1. Introduction

The behavior of magnetic impurities in a metallic host embraced in the well-known *Kondo effect* has been one of the most challenging problems in condensed matter physics [1]. This phenomenon is a fine example of development of electronic correlations in a solid, and in the last years it has witnessed a resurgence with the development of nanoelectronic devices and novel nanostructured materials [2, 3]. However, there is probably no other area where the presence of the *Kondo effect* is so fundamental as in

Breakdown of the coherence effects and Fermi liquid behavior in YbAl_3 nanoparticles

Strongly Correlated Electron Systems (SCES) (Ce-, U-, and Yb-based compounds) [4]. Within the existing theories, the *Kondo lattice model* [5] has been successfully applied for explaining the influence of *Kondo effect* on the physical properties of this kind of materials.

In the framework of this model, a large number of SCES can be classified as *Kondo lattice* systems, and these are viewed as a dense periodic array of magnetic ions, different to the single impurity systems, where the impurities are considered far away with no coherence between each other. The possibility that long range Fermi liquid coherence may break down in a Kondo alloy has open new perspectives since it may lead to the formation of non-trivial new quantum states [6, 7, 8]. Until now, this issue has mainly been experimentally explored for bulk materials by diluting the active Kondo ion with a non magnetic one (in Ce alloys), paying an especial attention to the crossover from *Kondo lattice* to single impurity regime detected by electrical resistivity measurements [9, 10, 11, 12, 13]. Less attention has been focused on Yb alloys respect to Ce systems, with only a few reports (see for instance [14, 15, 16]), where even this crossover hardly has been explored [17].

It is also remarkable to note that most of the reports in SCES have been constrained to macroscopically well-crystallized bulk materials. However it appears evident that the development of molecular beam epitaxy techniques have allowed very recently the production of two dimensional structures based on Ce-*Kondo lattice* systems, known as "Kondo superlattices" [18]. The reduction of the dimensionality results in new types of electronic states, as observed in CeIn_3 - LaIn_3 superlattices, where an enhancement of the effective electron mass and non Fermi liquid behavior were underlined [19]. Another example is the fabrication of multi-scale microstructures spanning from atomic to nanometer and mesoscopic scales in YbAl_3 alloy, showing a simultaneous enhancement of the electron and phonon transport properties [20].

Following this alternative route, novel phenomena appear when reducing the size of those materials to the nanometer scale. In particular, it is appealing to investigate deeper the eventual variations in the relation to the role of Kondo interaction, especially in *Kondo lattice* compounds [21]. There are only a few examples of experimental results on Ce alloys ([22, 23] and Refs. therein), and also some theoretical approaches (see for instance [24, 25, 26]). In Yb systems, a significant example is the nanosized YbAl_3 particles, which exhibits a decrease of the Yb valence with the size reduction. Such a decrease was attributed to the bonding loss of the surface atoms [27]. More recently, changes in the valence with the size reduction in REp_3 (RE=Eu, Yb) alloys were also observed [28]. For nanosized YbAl_3 , the bulk counterpart of this alloy is an archetypal intermediate valence system, which has been thoroughly studied in the past. The existence of energy scales related to coherence and Kondo effects allows to classify this alloy as a *Kondo lattice* system [14]. Electrical resistivity results indicate a decrease of the scattering around 100 K [29]. There is also a broad maximum around 100 K in the magnetic susceptibility and also in the magnetic contribution to the specific heat related to an energy scale (Kondo temperature ($T_K = 500$ -670 K)) [14, 30, 31], as found as well

Breakdown of the coherence effects and Fermi liquid behavior in YbAl_3 nanoparticles 3

in the nanosized YbAl_3 alloys [27]. In this kind of material with a Kondo temperature higher than 500 K, the crystalline field effects are found to play a secondary role [1, 14, 30, 32]. Moreover, studies on $\text{Yb}_{1-x}\text{Lu}_x\text{Al}_3$ series of alloys showed that according to magnetic susceptibility and specific heat measurements the appearance of a second energy scale at 40 K in the intermediate valence *Kondo lattice* YbAl_3 is a true coherence effect [14]. In addition, a reduction of *Kondo lattice* effects in $\text{Yb}_{1-x}\text{Lu}_x\text{Al}_3$ was observed by soft x-ray photoelectron spectroscopy with a behavior in a good agreement with the single impurity Anderson model [15]. However, it is interesting to note that details of these changes in the *Kondo lattice* behavior has not been explored so far by electrical resistivity ($\rho(T)$) measurements in this Yb-substituted series $\text{Yb}_{1-x}\text{Lu}_x\text{Al}_3$, despite it represents a smoking gun evidence to disclose the evolution of the coherence effects and the Kondo regime in strongly correlated Yb and Ce compounds. The Fermi liquid regime ($\propto T^2$) at low temperatures and coherence effects, hallmarks of a *Kondo lattice* behavior, can be easily identified by measuring electronic transport properties.

Considering the electronic properties of nanosized YbAl_3 [27] and those commented for the bulk alloy above, it is relevant to scrutinize the influence of the size reduction on the electronic transport properties (electrical resistivity), and how the *Kondo lattice* behavior and the Fermi liquid ground state (T^2 dependence at low temperatures) are affected, both constitute the main aims of this work. This will represent a definite step forward within SCES systems (Ce, Yb, U alloys). Additionally, the results are compared with that obtained for the non-magnetic reference LuAl_3 nanometric alloy, and with the dilution effect by nonmagnetic Lu in bulk YbAl_3 alloy using the electrical resistivity as well.

2. Experimental

Nanocrystalline LuAl_3 alloy was prepared by high-energy mechanical milling of a starting bulk alloy. Then, the alloy was crushed and milled in a planetary high-energy ball system (Retsch PM 400/2) at a rotation speed of 200 rpm, using a container and balls made of tungsten carbide, a similar procedure, as already used in the study of the YbAl_3 and other Rare Earth nanoalloys [27, 33]. The bulk $\text{Yb}_{0.2}\text{Lu}_{0.8}\text{Al}_3$ alloy was prepared in an arc furnace from constituent elements Yb (Alfa-4N), Lu (Alfa-4N) and Al (Alfa-5N). Transmission Electron Microscopy (TEM) was performed in a JEOL JEM 2100 microscope. X-ray diffraction measurements were performed at room temperature with a Bruker D8 Advance diffractometer using $\text{Cu-K}\alpha$ radiation. Electronic transport properties were measured by the four probe method in a Quantum Design PPMS device. For the electrical resistivity measurements the milled powder is first pressed in a press pellet die. A disk is then obtained, which has to be cut in a parallelepiped shape. The sample bar was of a typical length (10 mm) and area ($2 \times 2.5 \text{ mm}^2$). Our in-house holder consisted of 4 spring-loaded pins. The pin holder was screwed on top of the sample until a certain deformation was observed in the springs. The spring-loaded pins are rounded to secure an excellent contact.

3. Results

Figure 1 shows the X-ray diffraction patterns and results of Rietveld refinement of 70 h milled YbAl₃ (a) and LuAl₃ (b) alloys. The Rietveld analysis of x-ray data for 70 h milled YbAl₃ alloy (Bragg factor: $R_B = 10\%$) provided the unit-cell parameter $a = 4.2037(7)$ Å, mean grain size $D_{XRD} = 12(2)$ nm and lattice strain $\eta = 0.37(3)\%$, in agreement with the previously reported results [27]. For the sample LuAl₃ milled for 70 h, with a Bragg factor ($R_B = 7\%$), values of $a = 4.1918(4)$ Å, $D_{XRD} = 10(2)$ nm and $\eta = 0.64(3)\%$ are calculated. The structural characterization was completed collecting TEM images. Figure 1 (c) and (d) show representative high resolution transmission electron microscopy (HRTEM) images of the 70 h milled YbAl₃ and LuAl₃ nanoparticles. The figures show a single YbAl₃ particle with a mean diameter 14 nm diameter (Figure 1 (c)) and of 11 nm for LuAl₃ nanoparticle (Figure 1(d)). The lattice planes can be clearly observed, which indicates that the nanoparticles are crystalline in the core. These values of the mean size of the nanoparticles are near to those obtained by the analysis of the X-ray diffraction data.

Figure 2(a) shows the temperature dependence of the total electrical resistivity ($\rho(T)$) in bulk, 20 h, and 70 h milled YbAl₃ alloys. It is observed a gradual change in the high temperature slope in the milled samples respect to the bulk alloy, with a decrease of the relative variation in all temperature range with the milling process. For 70 h milled YbAl₃ alloy there are two important features that indicate a remarkable difference with the bulk sample: the high temperature slope, and a minimum around 15 K, as indicated by the marker, in more detail in figure 2(b). There is also a broad hump in the 70 h milled YbAl₃ alloy.

The appearance of this hump is typical in the magnetic contribution to $\rho(T)$ of intermediate valence *Kondo lattice* systems, as observed for instance in the intermediate valence YbCuAl [34]. When coming down from high temperatures in 70 h milled YbAl₃, the $\rho(T)$ increase can be attributed to the incoherent Kondo scattering (high temperature scale- $T_K = 670$ K [14]) until the decrease below $T_{max} = 125$ K. Thus, the contribution to the electrical resistivity in 70 h milled YbAl₃ (see Figure 2(b)) basically comes from the magnetic scattering and the residual resistivity terms. This suggests that the disorder provoked by the milling process induces an increase of the scattering from defects in the crystal lattice, starting to play a more significant role than the electron-phonon scattering. This fact has been observed in other milled Rare Earth-based alloys, where the electrical resistivity has shown a significant reduction of the high temperature slope with the increase of the milling time, with values of $RRR = \rho_{300K}/\rho_{4K}$ (Residual Resistivity Ratio) changing from 1.6 to 1.1 [35].

On the other hand, at low temperatures a drastic change (although relatively reduced) in the behavior is observed in such a milled sample respect to the bulk alloy, with a marked upturn and the presence of a minimum around 15 K, as shown in Figure 2(a,b). Precisely there is a small upturn in YbAl₃ 20 h ($\langle D_{XRD} \rangle \approx 19$ nm [27]) which demonstrates that the appearance of the minimum at 70 h alloy is not casual but the

1
2
3 *Breakdown of the coherence effects and Fermi liquid behavior in YbAl₃ nanoparticles* 5
4
5 result of a definite tendency (see Figure 2 (c)). The consequence of this minimum is a
6 deviation from standard Fermi liquid behavior, as shown in Figure 3, when comparing
7 the bulk and 70 h milled YbAl₃ alloy samples.

8
9 To analyze the origin of such a minimum in $\rho(T)$ it is pertinent to check $\rho(T)$ in
10 LuAl₃ milled for 70 h. This will allow to test whether the minimum is observed in a
11 conventional metallic alloy of a similar nanometric structure. In this case (see Figure
12 4 (a)), the shape of the resistivity curve is that of a typical metal. Curiously it also
13 displays a minimum, much shallower than that in 70 h milled YbAl₃, as shown in
14 details in the inset of Figure 4 (a). This last feature could be intuitively interpreted
15 as additional contributions around the minimum in the Yb-based alloy, which we will
16 commenting below.
17
18

19 The analysis of the different contributions to $\rho(T)$ in disordered (amorphous) metals
20 and nanocrystalline alloys is not a simple task. There exist several mechanisms that
21 could provide a reasonable interpretation for the increase of the electrical resistivity
22 at low temperatures for the nanometric 70 h milled YbAl₃ and LuAl₃ alloys. To
23 facilitate the interpretation we will describe our rationale step by step. Firstly, it could
24 be expected the low temperature upturn be due by eventual changes in the density
25 of carriers, which are considered commonly in semiconducting materials and hopping
26 conductivity. In a second step we will discuss quantum interference effects (QIE) usually
27 observed in compounds of amorphous nature [36, 37]. Finally, a third plausible approach
28 to quantify is the role of an eventual Kondo effect in the Yb sample will be discussed
29 as another extra scattering source frequently present in SCES Yb alloys.
30
31
32
33

34 Regarding the first mechanism, our $\rho(T)$ measurements indicated an ohmic
35 dependence (see Figure 4(b)), thus providing *a reasonable evidence for a metallic*
36 *conductivity*. Thus, ruling out the influence of oxides such as Yb₂O₃ in $\rho(T)$. The
37 presence of this oxide (less than 3 %) of the sample) has been previously detected
38 in bulk and milled YbAl₃ alloys [27]. Consequently, this ohmic dependence of $\rho(T)$
39 also eliminates the possibility of hopping conductivity, based on Mott metal-insulator
40 transition, with an exponential dependence anyway [38]. Secondly, an electrical
41 resistivity minimum has been widely observed in amorphous materials of high
42 ρ_0 ($\gtrsim 80 \mu\Omega\text{cm}$). The high-energy milling process usually leads to sizeable lattice
43 strains and deformations, thus giving rise to a poorly crystallized environment at a very
44 local range [39]. Therefore, it would not be surprising to detect an influence of these
45 effects in $\rho(T)$. Quantum electron interaction effects [36] put forward two corrections,
46 namely the electron-electron interaction (EEI) and the weak localization (WL). In the
47 following, we will briefly comment on both effects. Although EEI and WL introduce
48 temperature dependent corrections to resistivity, in three-dimensional disordered metals
49 at low temperatures, the contribution to resistivity from the EEI effects dominates over
50 that due to WL effects [36, 40]. Assuming the existence of EEI, the correction to
51 conductivity (σ) is derived as:
52
53
54
55
56
57

$$\Delta\sigma_{ee} = \frac{1.3}{\sqrt{2}} \frac{e^2}{2\pi h} F_0 \sqrt{\frac{2\pi k_B T}{hD'}} \quad (1)$$

58
59
60

Breakdown of the coherence effects and Fermi liquid behavior in YbAl_3 nanoparticles

where $D' = \frac{v_F^2 \tau}{3}$ is the diffusion constant, in terms of the Fermi velocity v_F and the relaxation time τ . F_0 is a screening term which turns to 4/3 in the case of the absence of an applied magnetic field. Experimental reports revealing the $\rho \propto -\sqrt{T}$ dependence have been extensively published for disordered metals [37]. On the other hand, the electron wave propagation, away from a classical interpretation, allows a variety of paths with the existence of loops of interference between the electron waves giving rise to a factual localization. If all particles returned back to the origin, then $\rho \rightarrow \infty$ and the full localization would be achieved.

An ideal approach to determine the influence of EEI effects is then to include $\rho \propto -\sqrt{T}$. As shown in Figure 5 (a), one can realize that it is possible to fit a linear variation (\sqrt{T} dependence) for 70 h milled LuAl_3 alloy. This supports experimentally the former assumption: the mechanism related to the electrical resistivity minimum in LuAl_3 is the commented quantum corrections.

Regarding the YbAl_3 nano (70 h milled alloy), the contribution below the minimum shows an extra contribution. Let us first consider that for $T < T_{min}$ there is a major contribution from QIE effects as occurs in LuAl_3 . The fit only considering the $-\sqrt{T}$ term is not satisfactory (see Figure 5(b)), thus suggesting the presence of another more important scattering mechanism(s). In SCES Yb systems we presented above there could exist a contribution stemming from the Kondo effect ($\rho \propto -\ln(T)$) [1]. In this sense, we have found that the low temperature data ($T < 7$ K), is well described according to the $-\ln T$ dependence, and the results are displayed in Figure 5 (c). This could indicate the presence of an additional temperature scale ($T^* = 7$ K) related to the onset of an eventual Kondo contribution at low temperatures, different to the high T_K temperature scale.

4. Discussion

The outcome of the former analysis is that the experimental evidence is explained by both QIE and Kondo interaction, which are responsible for the low temperature upturn below T_{min} . The milling of the bulk YbAl_3 results in an ensemble of nanoparticles randomly dispersed and in contact, forming a granular alloy. It is commonly accepted that nanoparticles can be generally described as a two-component system consisting of the core nanocrystallites and a grain or interphase boundary components [41]. The thickness of this grain boundary is commonly assumed around 1 nm. At grain boundaries, more disorder is expected in relation to the core of nanoparticles. On the one hand, the nanometric size of the particles favors the presence of surface shells in which the atomic coordination is reduced whereas the microstrain is enhanced. In this situation the nanostructure becomes more and more disordered, affecting the electrical resistivity. Therefore, such a considerable disorder is the basic element supporting the QIE.

In bulk YbAl_3 , the f -electron atoms are forming a periodic array which lie in the so-called *Kondo lattice* systems [5]. Every spin in the lattice is screened by the conduction

Breakdown of the coherence effects and Fermi liquid behavior in YbAl₃ nanoparticles 7

electrons. In real space, the screening takes place on a length scale of mesoscopic size ($\xi_K = \hbar v_F / k_B T_K$, where v_F is the Fermi velocity), denoted as the Kondo screening cloud [42]. The values of Fermi velocity may range from 10^6 m/s for normal metals to $10^3 - 10^4$ m/s in Heavy Fermion systems [43]. Consequently, the Fermi velocity is directly related with the electronic contribution to the specific heat (Sommerfeld coefficient (γ)). The value of $\gamma = 45$ mJ/molK² estimated from the specific heat data in bulk YbAl₃ is found to decrease down to 36 mJ/molK² for the 70 h milled YbAl₃ alloy [27]. Since a value of the Fermi velocity $v_F = 4 \cdot 10^4$ m/s, is observed for the bulk YbAl₃ [44], a simple scaling with the variation of the coefficient γ leads to an appraisal of $5 \cdot 10^4$ m/s for the Fermi velocity in the milled sample. On the other hand, from the maximum in the magnetic susceptibility and magnetic contribution to the specific heat in bulk and milled YbAl₃ alloys [27], the T_K values do not change significantly, being around 500 K-670 K, as estimated for the bulk sample [14, 30, 32]. Thus, following the above reasoning, it is possible to estimate a value of ξ_K around 0.7 nm for the 70 h milled YbAl₃ alloy. The length scale ξ_K would be less than the mean size of our samples (12 nm), and consequently the Kondo screening cloud is restricted within the nanoparticle, at least in the core, with variations at the surface of the nanoparticles. The size effect would not be essential for the disruption of the Kondo lattice behavior, as the characteristic length is one order of magnitude lower than the mean grain size, whereas the increase in the lattice strain and the disorder at the surface of the particles with the size reduction process will play a significant role. Our measurements of electrical resistivity of nanosized YbAl₃ indicate that the nanoparticle ensemble provokes the breakdown of the *Kondo lattice* coherence, with a presence of a low temperature upturn.

It has been shown that the reduction of size in nano-YbAl₃ results in the Yb valence reduction as a consequence of the increasing non-magnetic Yb²⁺ atoms at the surface of nanoparticles [27]. Irrespective of this qualitative interpretation, what is clear is that by reducing the size, a $\rho(T)$ minimum appears with the low temperature upturn. As a matter of fact, this situation resembles the cases of bulk alloys under chemical substitution in which by adding non-magnetic rare-earth atoms (Y and La for Ce-based and La or Lu for Yb-based compounds) the transition from *Kondo Lattice* to single impurity regime is observed (see for instance [12, 17]). In bulk YbAl₃ the coherence scattering is maintained throughout the alloy as a result of a *Kondo lattice* behavior. This is greatly modified whenever there is a reduction of size and a concomitant increase of surface strain and disorder in the nanoparticle shell. For comparison purposes, the possibility of a change of regime by Lu dilution was explored in the bulk YbAl₃. The bulk sample Yb_{0.2}Lu_{0.8}Al₃ is found to crystallize in the same type of structure and space group *Pm-3m* as YbAl₃ and LuAl₃ alloys but with a lattice parameter $a = 4.1932(2)$ Å. The results show the presence of a low temperature minimum in $\rho(T)$ of the bulk Yb_{0.2}Lu_{0.8}Al₃ alloy with an upturn following a $-\ln T$ dependence (see Figure 6). Curiously, the position of this minimum around 7 K, coincides with the onset of $-\ln T$ term below the temperature scale T^* , associated to the low temperature upturn in the 70 h milled YbAl₃ alloy. Consequently, it is possible to find some similarities

Breakdown of the coherence effects and Fermi liquid behavior in YbAl_3 nanoparticles

between the size reduction and chemical substitution process by Lu in bulk YbAl_3 alloy. In both of cases there is an increase in the fraction of non-magnetic atoms (Yb^{2+} or Lu) and the disorder leading to a limit situation where the periodicity of the Kondo ions is broken. Consequently, a deviation from the Fermi liquid regime is observed.

Concerning the observed $-\ln T$ dependence of the low temperature upturn in the 70 h milled YbAl_3 alloy, it is obvious that the electronic transport in an ensemble of nanoparticles is complex. It will require further study in order to ascribe it to a Kondo behavior.

5. Conclusions

It is concluded that the size in intimate combination with the increasing strain is a magnificent driving parameter, now for intrinsic electronic scattering changes. In this sense and to extend the universality of the former assert, it is widely known that particles of noble metals in nanocrystalline state can suffer serious changes in the density of states, as have been recently reported [45]. Therefore, our finding is naturally connected with a more general physical situation.

To summarize, the scrutiny of the electrical resistivity in nano- YbAl_3 particles has revealed a deviation from the Fermi liquid behavior at low temperatures. Such a deviation is due to the combined effect of the disruption of the periodicity of the Kondo ions as consequence of size reduction process and QIE favored by the presence of a disordered collection of nanoparticles.

6. Acknowledgements

This work was supported by the Spanish MINECO under project MAT2014-55049-C2-R.

- [1] Hewson A C 1997 *The Kondo problem to Heavy fermions* (Cambridge, England: Cambridge University Press)
- [2] Goldhaber-Gordon D, Shtrikman H, Mahalu D, Abusch-Magder D, Meirav U and Kastner M A 1998 *Nature* **391** 156
- [3] Prüser H, Dargel P E, Bouhassoune M, Ulbrich R G, Pruschke T, Lounis S and Wenderoth M 2014 *Nat. Commun.* **5** 5417
- [4] Coleman P 2007 *Handbook of Magnetism and Advanced Magnetic Materials* (Chichester: Wiley)
- [5] Doniach S 1977 *Physica B* **91** 231
- [6] Burdin S and Fulde P 2007 *Phys. Rev. B* **76** 104425
- [7] Kaul R K and Vojta M 2007 *Phys. Rev. B* **75** 132407
- [8] Burdin S and Lacroix C 2013 *Phys. Rev. Lett.* **110** 226403
- [9] Lawrence J M, Graf T, Hundley M F, Mandrus D, Thompson J D, Lacerda A, Torikachvili M S, Sarrao J L and Fisk Z 1996 *Phys. Rev. B* **53** 12559
- [10] Bud'ko S L, Fontes M B and Baggio-Saitovitch E M 1998 *J. Phys.: Condens. Matter* **10** 8815
- [11] Chudinov S, Brando M, Marcelli A and Battisti M 1998 *Physica B* **244** 154
- [12] Medina A N, Rojas D P, Gandra F G, Azanha W R and Cardoso L P 1999 *Phys. Rev. B* **59**(13) 8738
- [13] Pikul A P, Stockert U, Steppke A, Cichorek T, Hartmann S, Caroca-Canales N, Oeschler N, Brando M, Geibel C and Steglich F 2012 *Phys. Rev. Lett.* **108** 066405

- 1
2
3 *Breakdown of the coherence effects and Fermi liquid behavior in YbAl₃ nanoparticles* 9
4
5 [14] Bauer E D, Booth C H, Laurence J M, Hundley M F, Sarrao J L, Thompson J D, Riseborough
6 P S and Ebihara T 2004 *Phys. Rev. B* **69** 125102
7 [15] Yamaguchi J, Sekiyama A, Imada S, Yamasaki A, Tsunekawa M, Muro T, Ebihara T, Onuki Y
8 and Suga S 2007 *New J. Phys.* **9** 317
9 [16] Köhler U, Oeschler N, Steglich F, Maquilon S and Fisk Z 2008 *Phys. Rev. B* **77**(10) 104412
10 [17] Rojas D P, Medina A N, Gandra F G, Fernández Barquín L and Gómez Sal J C *in press Physica*
11 *B*
12 [18] Shimozawa M, Goh S K, Shibauchi T and Matsuda Y 2016 *Reports on Progress in Physics* **79**
13 074503
14 [19] Shishido H, Shibauchi T, Yasu K, Kato T, Kontani H, Terashima T and Matsuda Y 2010 *Science*
15 **327** 980
16 [20] He D, Zhao W, Mu X, Zhou H, Wei P, Zhu W, Nie X, Su X, Liu H, He J and Zhang Q 2017
17 *Journal of Alloys and Compounds* **725** 1297 – 1303
18 [21] Lonzarich G, Pines D and feng Yang Y 2017 *Reports on Progress in Physics* **80** 024501
19 [22] Chen Y Y, Huang P H, Ou M N, Wang C R, Yao Y D, Lee T K, Yao M Y, Laurence J M and
20 Booth C H 2007 *Phys. Rev. Lett.* **98** 157206
21 [23] Mohanta S K, Mishra S N, Iyer K K and Sampathkumaran E V 2013 *Phys. Rev. B* **87**(12) 125125
22 [24] Thimm W B, Kroha J and von Delft J 1999 *Phys. Rev. Lett.* **82** 2143
23 [25] Hand T, Kroha J and Monien H 2006 *Phys. Rev. Lett.* **97** 136604
24 [26] Schwabe A, Gütersloh D and Potthoff M 2012 *Phys. Rev. Lett.* **109** 257202
25 [27] Rojas D P, Barquín L F, Espeso J I and Rodríguez Fernández J 2008 *Phys. Rev. B* **78** 094412
26 [28] Subbarao U, Sarkar S, Jana R, Bera S S and Peter S C 2016 *Inorganic Chemistry* **55** 5603–5611
27 [29] Rowe D M, Kuznetsov V L, Kuznetsova L A and Min G 2002 *J. Phys. D: Appl. Phys.* **35** 2183
28 [30] Cornelius A L, Laurence J M, Ebihara T, Riseborough P S, Booth C H, Hundley M F, Pagliuso
29 P G, Sarrao J L, Thompson J D, Jung M H, Lacerda A H and Kwei G H 2002 *Phys. Rev. Lett.*
30 **88** 117201
31 [31] Burdin S, Georges A and Grepel D R 2000 *Phys. Rev. Lett.* **85** 1048
32 [32] Ebihara T, Bauer E D, Cornelius A L, Laurence J M, Harrison N, Thompson J D, Sarrao J L,
33 Hundley M F and Uji S 2003 *Phys. Rev. Lett.* **90** 166404
34 [33] Rojas D P, Barquín F, Fernández J R, Espeso J I and Sal J C G 2007 *Journal of Physics: Condensed*
35 *Matter* **19** 186214
36 [34] Schlottmann P 1989 *Physics Reports* **181** 1
37 [35] Echevarria-Bonet C, Rojas D P, Espeso J I, Fernández J R, de la Fuente Rodríguez M, Barquín
38 L F, Fernández L R, Gorria P, Blanco J A, Fdez-Gubieda M L, Bauer E and Damay F 2015
39 *Journal of Physics: Condensed Matter* **27** 496002
40 [36] Lee P A and Ramakrishnan T V 1985 *Rev. Mod. Phys.* **57** 287
41 [37] Howson M A and Gallagher B L 1988 *Phys. Reports* **170** 265
42 [38] Kittel C 1986 *Introduction to Solid State Physics* (New York: John Wiley & Sons)
43 [39] Echevarria-Bonet C, Rojas D P, Espeso J I, Rodríguez Fernández J, Rodríguez Fernández L, Gorria
44 P, Blanco J A, Fdez-Gubieda M L, Bauer E, André G and Fernández Barquín L 2013 *Phys.*
45 *Rev. B* **87**(18) 180407
46 [40] Ghosh T, Fukuda T, Kakeshita T, Kaul S N and Mukhopadhyay P K 2017 *Phys. Rev. B* **95**(14)
47 140401
48 [41] Rojas D P, Barquín L F, Fernández J R, Fernández L R and Gonzalez J 2010 *Nanotechnology* **21**
49 445702
50 [42] Park J, Lee S S B, Oreg Y and Sim H S 2013 *Phys. Rev. Lett.* **110**(24) 246603
51 [43] Mourachkine A 2004 *Room-temperature Superconductivity* (Cambridge, UK: Cambridge
52 International Science Pub.)
53 [44] Demsar J, Kabanov V V, Alexandrov A S, Lee H J, Bauer E D, Sarrao J L and Taylor A J 2009
54 *Phys. Rev. B* **80**(8) 085121
55 [45] Garitaonandia J S, Insausti M, Goikolea E, Suzuki M, Cashion J D, Kawamura N, Ohsawa H,
56
57
58
59
60

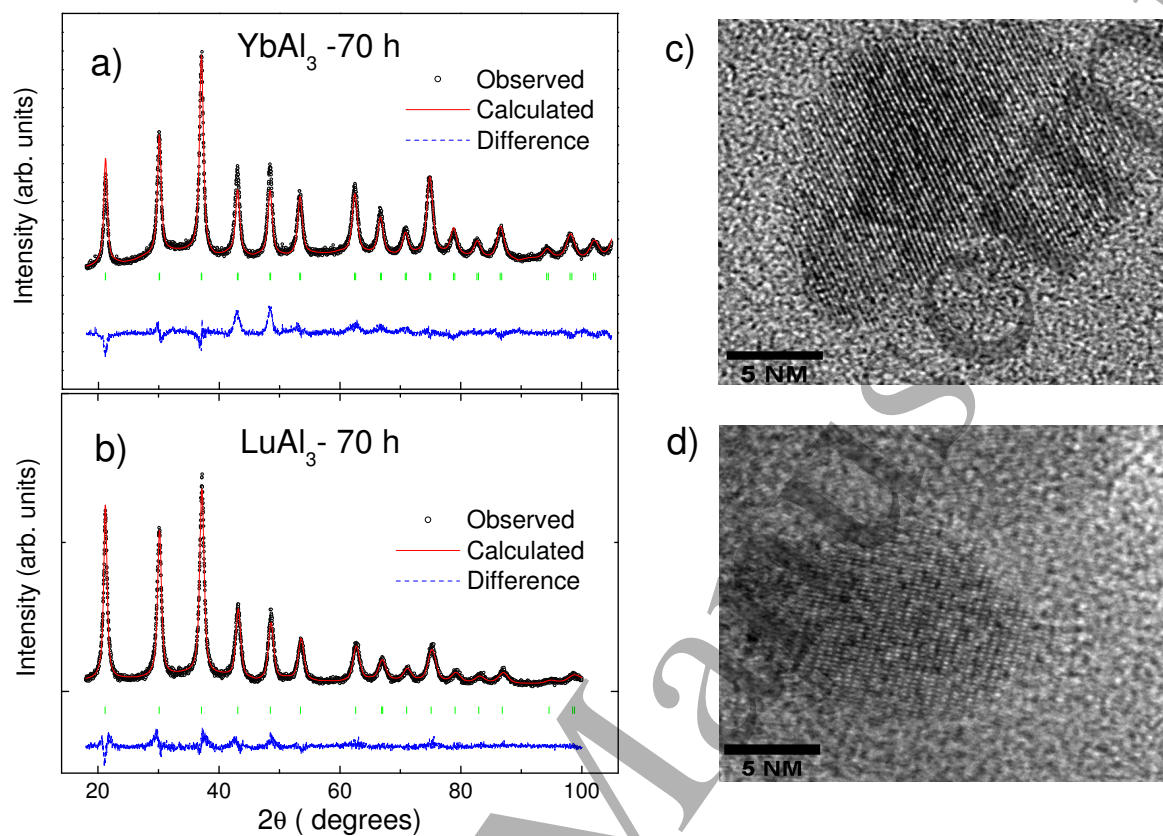
Breakdown of the coherence effects and Fermi liquid behavior in YbAl_3 nanoparticles¹⁰

Figure 1. X-ray diffraction patterns and results of Rietveld refinement of 70 h milled YbAl_3 (a) and LuAl_3 (b) alloys. The vertical markers are the expected Bragg positions according to $Pm\bar{3}m$ space group. High resolution TEM image of a nanoparticle of 70 h milled YbAl_3 (c) and LuAl_3 (d) alloys.

Gil de Muro I, Suzuki K, Plazaola F and Rojo T 2008 *Nano Lett.* 8 661

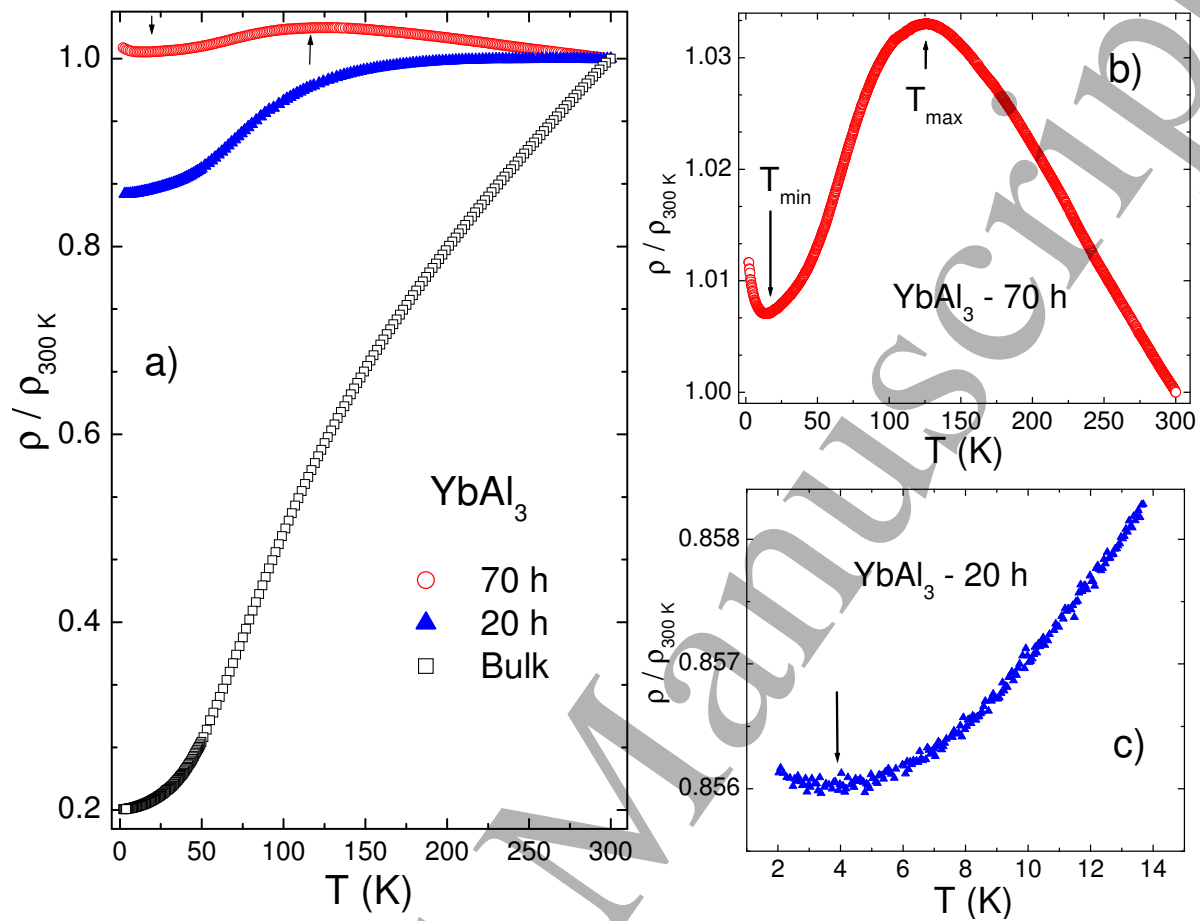
Breakdown of the coherence effects and Fermi liquid behavior in YbAl_3 nanoparticles¹¹

Figure 2. a) Normalized electrical resistivity vs temperature for bulk, 20 h and 70 h milled YbAl_3 alloys. In the milled sample, there is a minimum followed by an increase of the resistivity, up to a broad maximum, as indicated by the markers. b) Details of normalized electrical resistivity curve for 70 milled YbAl_3 alloy, highlighting the existence of a temperature minimum and maximum. c) Details of the low temperature region of 20 h YbAl_3 milled alloy showing a minimum in $\rho(T)$ around 4 K.

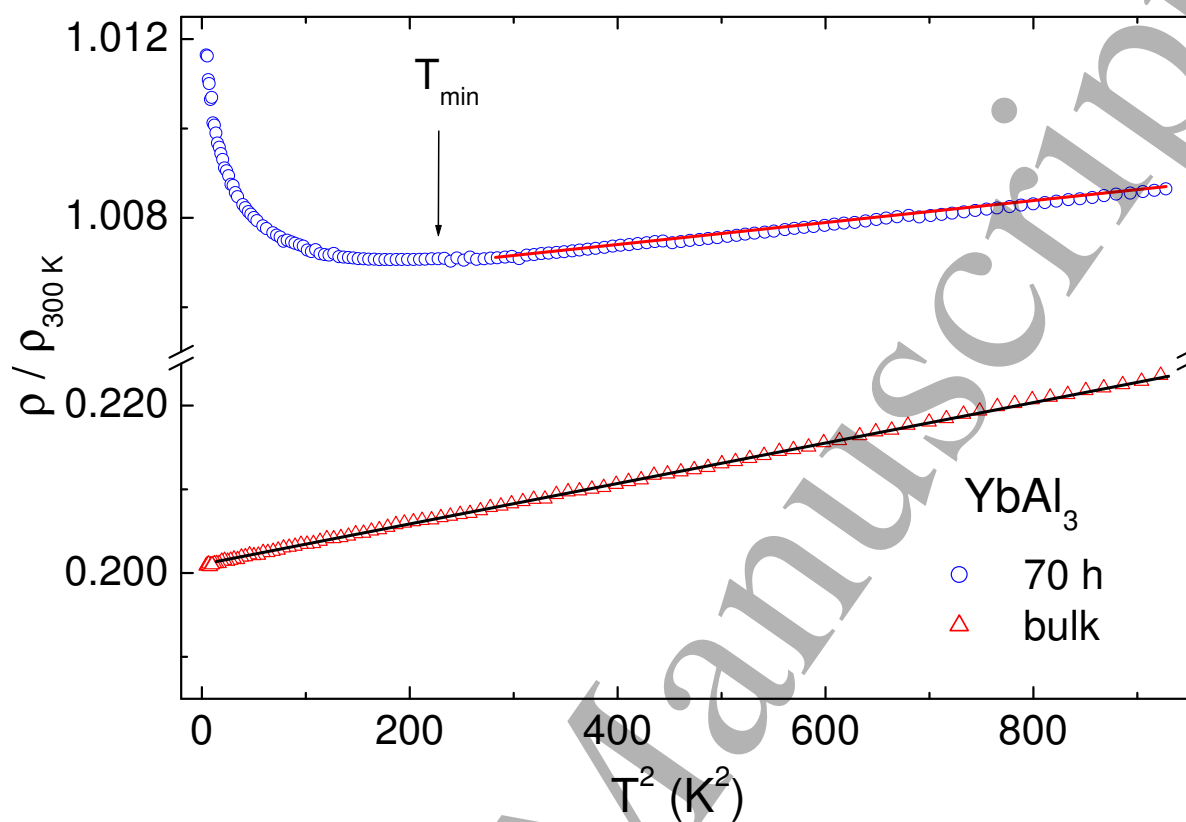
Breakdown of the coherence effects and Fermi liquid behavior in YbAl_3 nanoparticles¹²

Figure 3. Details of the low temperature region of bulk and 70 h milled YbAl_3 alloys showing a deviation from the Fermi liquid dependence below T_{min} in the nanometric alloy.

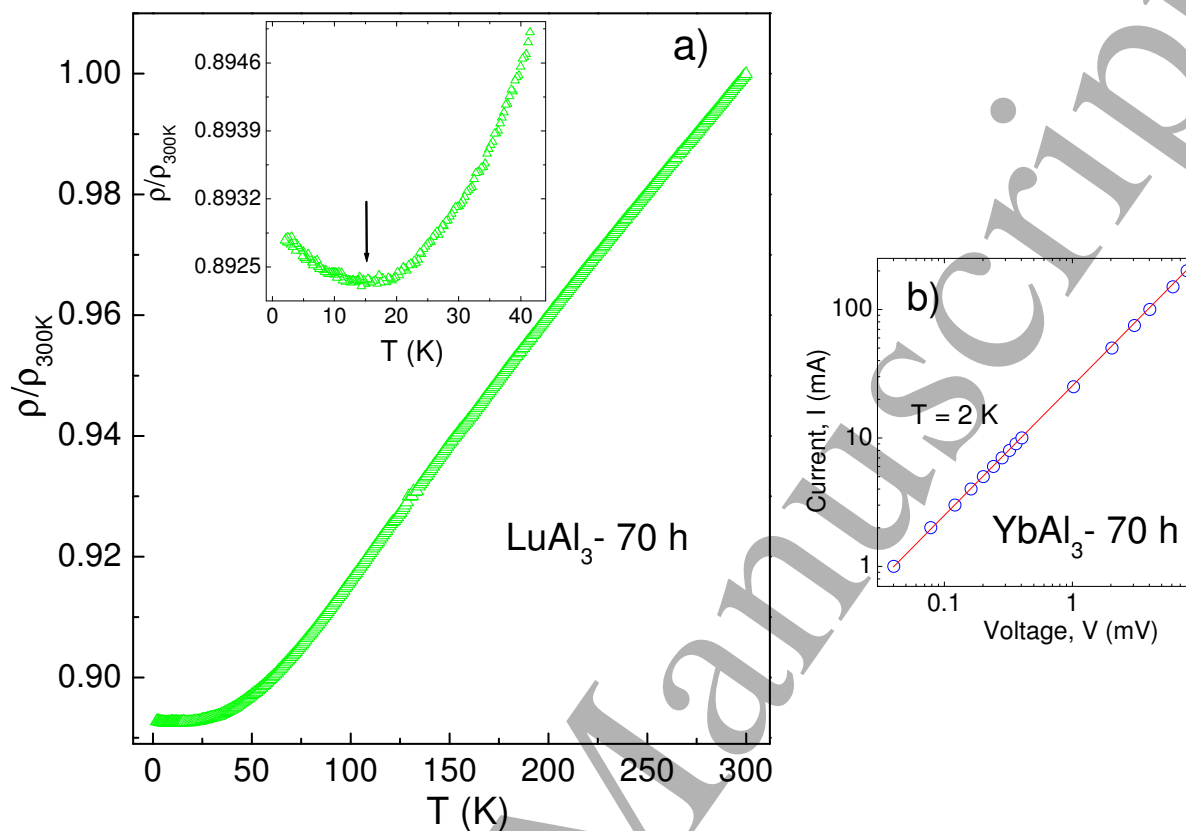
Breakdown of the coherence effects and Fermi liquid behavior in YbAl_3 nanoparticles¹³

Figure 4. a) Normalized electrical resistivity curve of the 70 milled LuAl_3 alloy. The inset details the low temperature region showing the presence of a minimum around 15 K. b) Curve of applied current (I) vs. voltage (V) in log-log scale at 2 K in the 70 h milled YbAl_3 alloy.

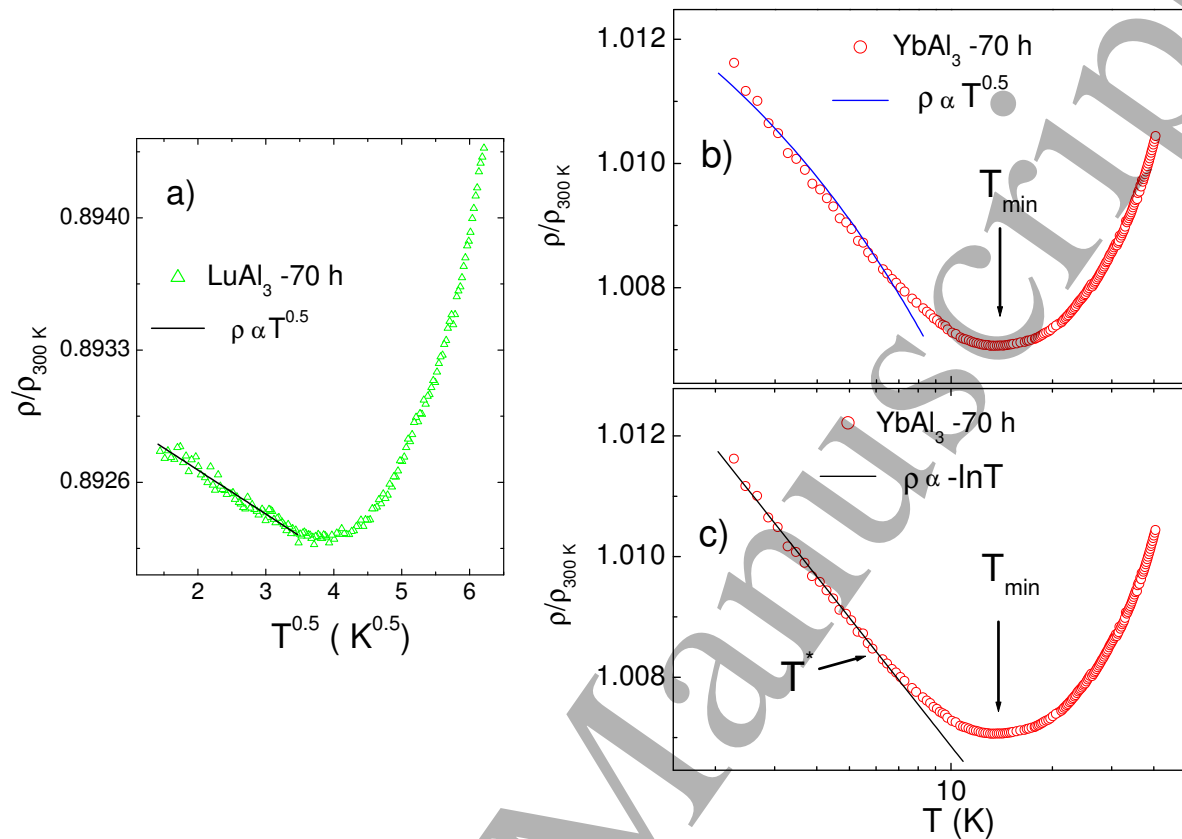
Breakdown of the coherence effects and Fermi liquid behavior in YbAl_3 nanoparticles¹⁴

Figure 5. a) Low temperature region of electrical resistivity described by a $-\sqrt{T}$ term in 70 h milled LuAl_3 . Fitting of the electrical resistivity data in 70 h milled YbAl_3 alloy in logarithmic scale, according to $-\sqrt{T}$ term (b) and a $-\ln T$ dependence (c). In the Yb alloy, the data is better described by a $-\ln T$ behavior below $T^* = 7$ K.

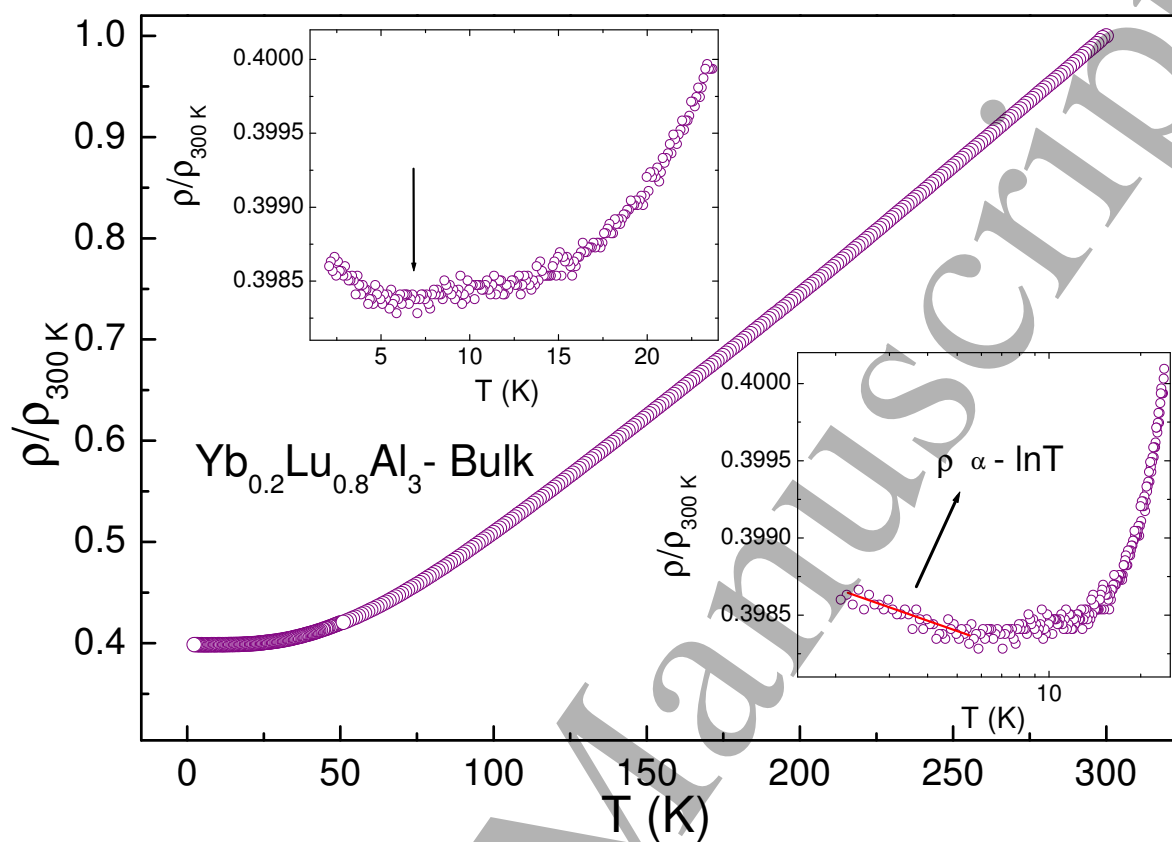
Breakdown of the coherence effects and Fermi liquid behavior in YbAl_3 nanoparticles¹⁵

Figure 6. Normalized electrical resistivity curve of $\text{Yb}_{0.2}\text{Lu}_{0.8}\text{Al}_3$ bulk alloy. Details of the low temperature region showing the presence of a minimum around 7 K (left inset), with an upturn according to $-\ln T$ dependence (right inset).